10-3-2012

Infrared thermography for noninvasive real-time monitoring of HIFU ablation

Yi-Sing Hsiao
University of Michigan

Ronald Kumon
Kettering University

Cheri X. Deng
University of Michigan

Infrared Thermography for Noninvasive Real-Time Monitoring of HIFU Ablation

Yi-Sing Hsiao, Ronald E. Kumon, and Cheri X. Deng

Department of Biomedical Engineering, University of Michigan
2200 Bonisteel Blvd., Ann Arbor, MI 48109-2099, USA

Abstract. Infrared imaging for spatiotemporal temperature measurements was explored in this study for non-contact monitoring of temperature increases generated by HIFU ablation. Using ex vivo cardiac tissue specimens, we investigated the correlations between the occurrence of events during HIFU ablation (e.g., lesion formation, cavity formation) and the 2D spatiotemporal temperature of the tissue surface measured during HIFU ablation from an infrared camera. An increase in the rate of temperature rise was observed when lesions formed at or slightly beneath the tissue surface. Spatial shifts in the maximum temperature location away from the HIFU focus were often observed with continuing HIFU exposure after lesion formation, suggesting tissue dehydration and cavitation formation during ablation with excessive heating.

Keywords: HIFU Ablation; Infrared Thermography; Lesion Monitoring
PACS: 43.80.Sh, 85.60.Gz, 87.50.Y-

INTRODUCTION

Monitoring tissue temperature during high-intensity focused ultrasound (HIFU) provides information to assess coagulative necrosis and helps to prevent overheating which can initiate gas bubble formation and cavitation. Infrared (IR) thermography, capable of non-contact, real-time monitoring of surface temperature with high temporal and spatial resolution, has been utilized to measure temperature rise during HIFU exposures [1-3]. However in these studies, either only phantoms were used, a temperature threshold was set to correlate with lesion formation, or only the temperature rise at a few locations was reported. In this study, we investigated the spatiotemporal temperature changes obtained with IR imaging and their correlation with relevant events during HIFU ablation (e.g., lesion formation, cavity formation).

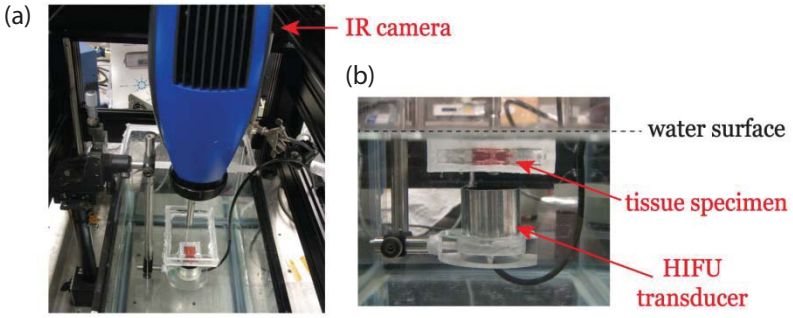

FIGURE 1. (a) The experimental setup with IR camera mounted on top of the tissue specimen. (b) The surface of the tissue specimen was above water to allow IR measurements.

11th International Symposium on Therapeutic Ultrasound
AIP Conf. Proc. 1481, 143-148 (2012); doi: 10.1063/1.4757325

METHODS AND MATERIALS

Experiments. HIFU experiments were performed with a focused transducer (3.98 MHz center frequency, $F = 1$) submerged in water facing up towards a freshly-excised porcine cardiac tissue specimen. The top surface of the specimen was above the water level to allow temperature measurements using an IR camera (Silver 5600, FLIR Systems, Boston, MA, USA) (Fig. 1.). HIFU exposures and IR imaging acquisition were synchronized by simultaneously recording their trigger signals (OMB-DAQ-3000, Omega Engineering, Stamford, CT, USA). Two-dimensional (2D) temperature images were recorded at a 50 Hz frame rate. Bright-field imaging, which was also synchronized with IR imaging and HIFU exposures, was performed using a video camera at 24 Hz frame rate (D5000, Nikon, Melville, NY, USA) to monitor the tissue surface and identify lesion, cavity formation, and tissue dehydration (water coming out of tissue) due to the HIFU exposure.

Emissivity of porcine cardiac tissue for IR temperature calibration was measured using the black tape method [4], with the Scotch Super 33+ Vinyl Electrical Tape (3M Company, St. Paul, MN, USA) with a known emissivity of 0.95.

Analysis. The surface temperature of the tissue obtained with IR imaging was analyzed to determine the temporal rate of temperature change at a given spatial location (x, y) and time t by

$$\text{Rate of Temperature Change} = \frac{\partial T(x, y, t)}{\partial t}.$$

In cases where lesions formed at the surface, bright-field images of the tissue surface were compared with the images of the temperature and the rate of temperature change. The temperature data were used to calculate the Arrhenius damage integral using 128 minutes as the cumulative equivalent minutes at 43°C (CEM_{43}) [5]. Lesion growth predicted from the damage integral was compared to the measurements of lesion extent obtained from the bright-field images.

RESULTS

The emissivity of porcine cardiac tissue was measured to be 0.857 ± 0.006. Emissivity was therefore set to 0.86 for temperature measurements of all experiments in this study.

Sub-ablative HIFU Exposures

An initial set of experiments was performed using low HIFU intensities (e.g. 125 W/cm^2) to avoid generating tissue necrosis. The temperature profiles and the rate of temperature change obtained in the IR measurements (Fig. 2) exhibit the expected spatiotemporal increase of temperature, as predicted by the bio-heat equation, without lesion or bubble formation. As shown in Fig. 2b, the rate of temperature change was largest at the start of HIFU exposure and decreased over time, corresponding to an initial rapid temperature increase and subsequent slower rise.

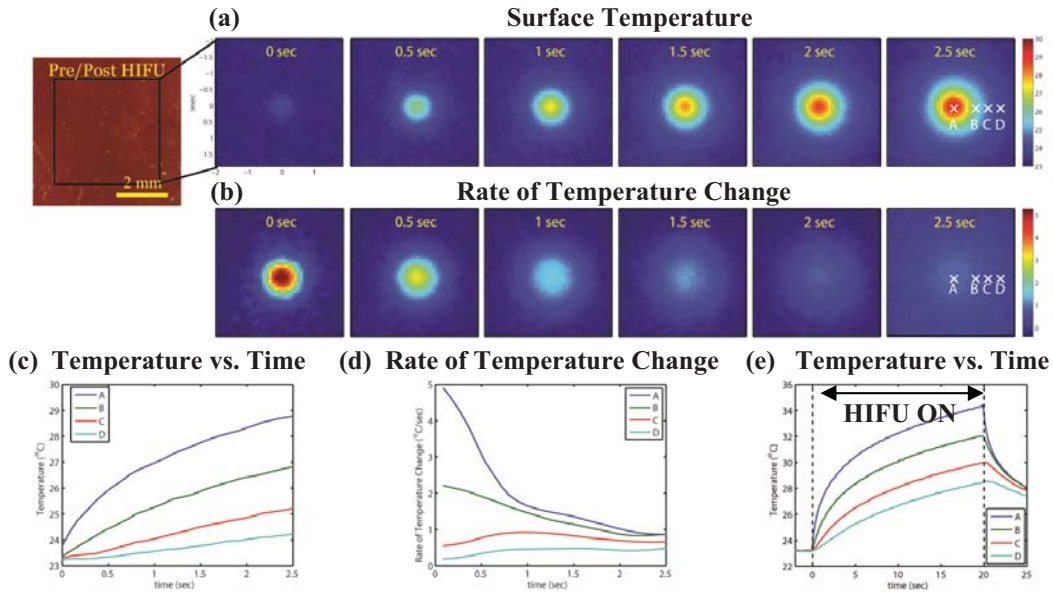

FIGURE 2. Sub-ablative HIFU exposures: (a) 2D temperature at t = 0 to 2.5 s recorded during a 20 s continuous HIFU exposure at 125 W/cm^2, with the focus placed at the surface. (b) The corresponding 2D rate of temperature change. (c) The temperature vs. time curve and (d) the rate of temperature change vs. time at A, B, C, D points shown in the right-most image in (a). (e) The temperature over the entire HIFU exposure.

Ablative HIFU Exposures

Ablation Focus near the Tissue Surface

When HIFU exposure was focused on the tissue surface, the time-resolved IR imaging revealed that the temperature initially followed the typical, expected profile after HIFU was applied. However, the temperature exhibited a more rapid increase (Figs. 3a, 3b, 3c) when a lesion was observed to form from the synchronized bright-field imaging, deviating from the smooth profile without lesion formation (Fig. 2e). This indicates an increase in the rate of temperature change, in contrast to the decreasing rate of temperature change prior to lesion formation (Figs. 3b, 3d, 3e).

With continual heating at sufficient HIFU intensity (e.g., 1060 W/cm^2), cavity was observed to form at the center of the lesion. Pockets of water then appeared near the lesion and cavity. This release of water from the tissue is most likely associated with tissue dehydration caused by HIFU heating. These events were identifiable in the IR temperature images as abnormal, erratic behaviors significantly deviating from the continuous and smooth profile (Fig. 4a).

In the data set shown in Fig. 3 and 4, the final surface lesion area measured from the bright-field image was 4.043 mm^2. The final surface lesion size computed from the damage integral using CEM_{43} = 128 minutes was 6.764 mm^2. The overestimated theoretical calculation (by 67.3%) is likely due to the lack of accurate consideration of cavity formation as well as dehydration.

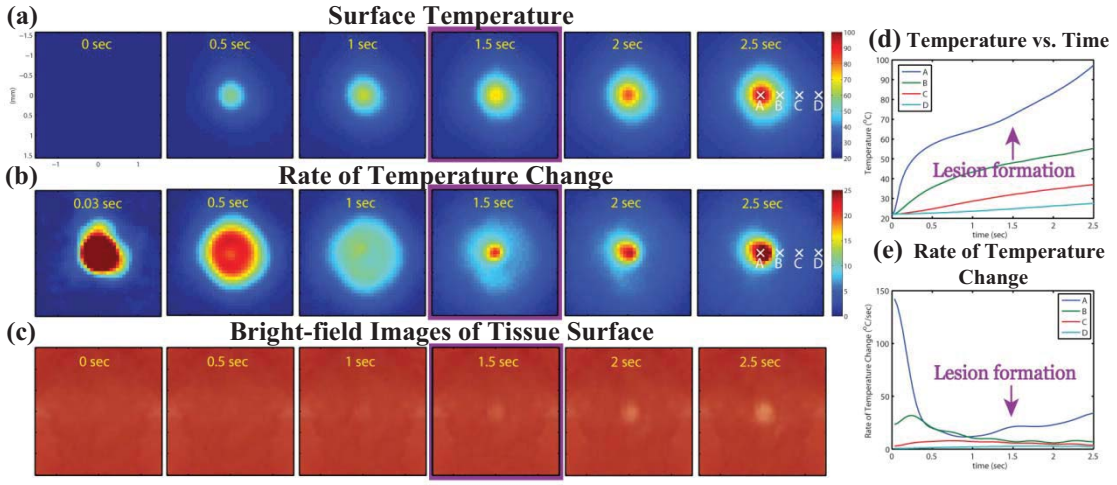

FIGURE 3. Ablative HIFU exposures with surface lesion formation: (a) 2D temperature at $t = 0$ to 2.5 s recorded during a 20 s continuous HIFU exposure at 1060 W/cm^2, with the focus placed at the surface. (b) The corresponding 2D rate of temperature change. Increases in the rate of temperature change started at 1.5 s. (c) The bright-field images of the tissue surface. Lesion started to form at 1.5 s. (d) The temperature vs. time curve and (e) the rate of temperature change vs. time at A, B, C, D points shown in the right-most image in (a).

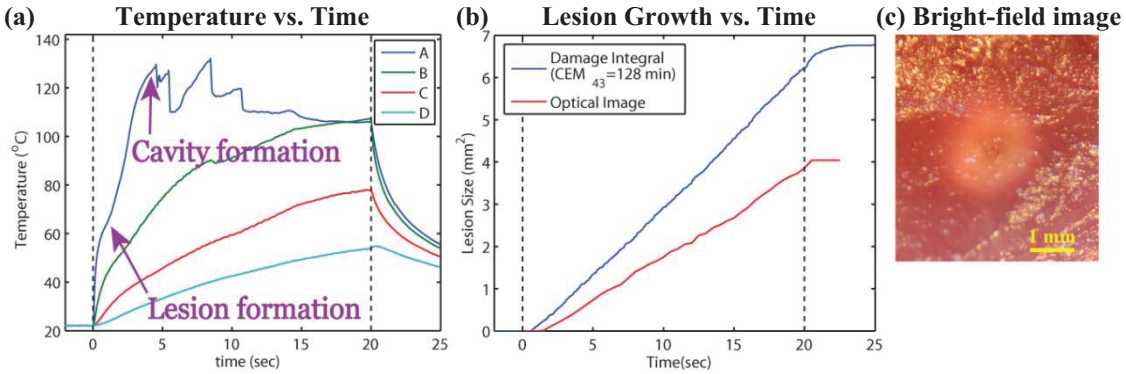

FIGURE 4. Ablative HIFU exposures with surface lesion formation (same set of data as in Fig. 3): (a) The temperature vs. time curve at A, B, C, D points shown in the right-most figure in Fig. 3a. The lesion formation and cavity formation time was identified from the bright-field images. (b) Comparison of lesion growth from the bright-field images and the damage integral results. (c) The bright-field images of the end lesion. A cavity can be seen in the center of the lesion.

Sub-Surface Ablation

When HIFU with intensity level capable of generating tissue necrosis was focused beneath the surface, an abrupt increase in the rate of temperature rise was also observed, suggesting the start of sub-surface lesion formation (Fig. 5).

With continual HIFU exposure, the location of the spatial maximum temperature appeared to shift away from its original central location (Fig. 6a), followed by the "rise-plateau-rise" type profile (Fig. 6c), similar to the cases with surface ablation (Fig. 5) where cavity formation and tissue dehydration were observed. Lesions observed in the gross images in these cases appeared to exhibit the typical discolorization within the lesion core (i.e. grayish yellow vs. the usual pink/white discolorization observed in lesions with less intense HIFU) that may be associated

with overheating. The over-cooked lesions sometimes also have a sponge- or foam-like appearance. The overheating may be related to excessive temperature increase accompanied by gas bubble formation and cavitation, as well as tissue dehydration.

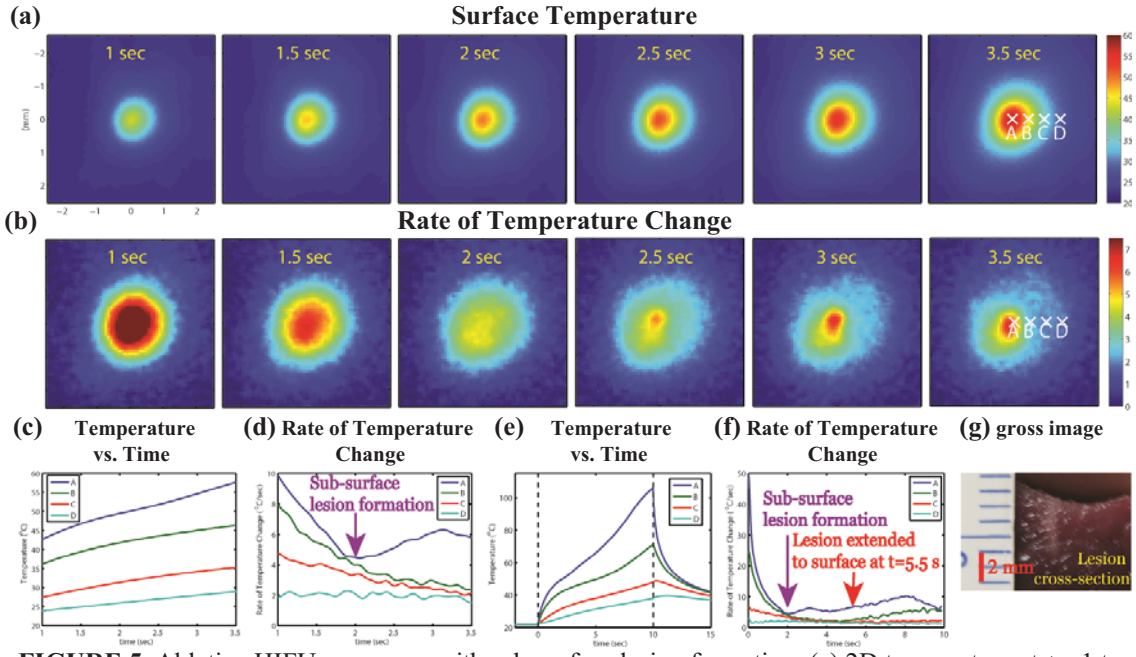

FIGURE 5. Ablative HIFU exposures with sub-surface lesion formation: (a) 2D temperature at t = 1 to 3.5 s recorded during a 10 s continuous HIFU exposure at 1060 W/cm^2, with the focus placed at 3 mm beneath surface. (b) The corresponding 2D rate of temperature change. Increases in the rate of temperature change started at 2 s. No lesion was formed at the surface at this time. (c) The temperature vs. time curve and (d) the rate of temperature change vs. time at A, B, C, D points shown in the right-most image in (a). (e) The temperature vs. time over the entire HIFU exposure time. (f) The rate of temperature rise vs. time over the entire HIFU exposure time. (g) Final gross tissue image.

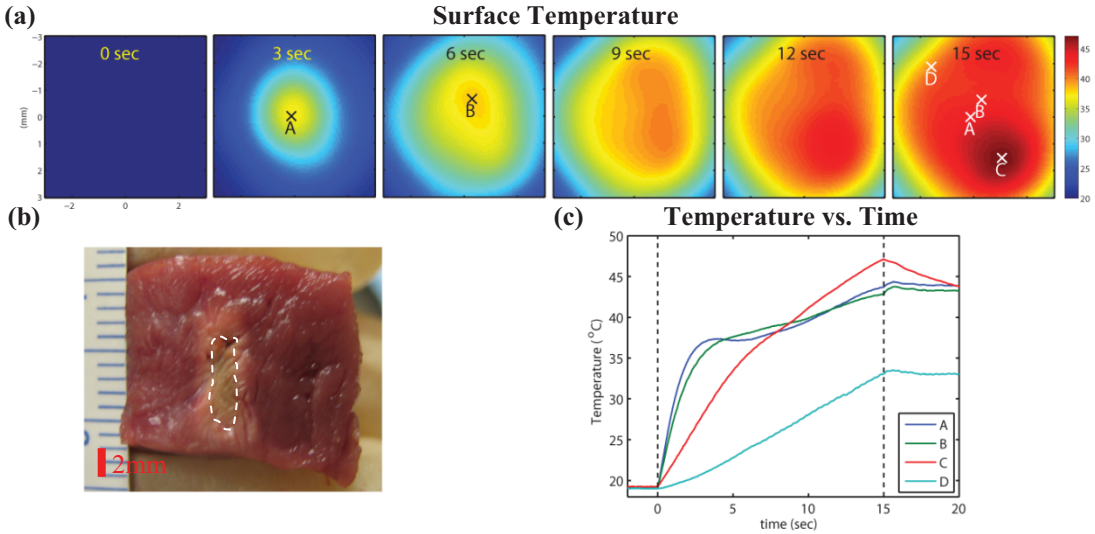

FIGURE 6. Ablative HIFU exposures with sub-surface lesion formation: (a) 2D temperature recorded during a 15 s continuous HIFU exposure at 1860 W/cm^2, with the focus placed at 8 mm beneath surface. (b) Gross tissue showing overcooked lesion in the center, indicated by the white dotted lines. (c) The temperature vs. time curve at A, B, C, D points shown in the right-most image in (a).

DISCUSSION AND CONCLUSIONS

The rate of temperature change is the highest immediately after HIFU is started, and decreases quickly as HIFU continues, corresponding to the initial rapid HIFU absorption followed by a slower increase as heat is conducted away into the surrounding tissue. A reversal of the rate of temperature change, or the increase in the rate of temperature change instead of the continuing decrease during HIFU ablation was observed to correlate with lesion formation. This increase can be explained by the increase in attenuation coefficient of the necrotized tissue in the lesion as compared to the normal tissue [6], resulting in an increase of the energy absorption. Erratic changes in the spatiotemporal temperatures at the surface also identified cavity formation and tissue dehydration, as verified by bright-field imaging. These characteristic behaviors were also observed in the sub-surface ablation experiments. In addition, shifting of the spatial maximum temperature point from its original central location in the sub-surface ablation experiments was observed, suggesting tissue overheating, which may be due to bubble formation, cavitation, and/or tissue dehydration. These events are stochastic in nature and can cause the observed 2D temperature field to change from being axially symmetric to a somewhat random spatial pattern.

In this study, our experimental results demonstrated that the spatiotemporal changes of temperature measured at the tissue surface by non-contact, real-time IR imaging can identify characteristic changes of temperature corresponding to lesion formation, cavity generation, as well as tissue dehydration during HIFU ablation. Studies to further investigate the correlation of spatiotemporal changes of surface temperature with subsurface ablation outcomes are ongoing to identify the relevant parameters and to establish the spatial and temporal resolution and sensitivity of IR imaging for monitoring HIFU ablation processes.

ACKNOWLEDGMENTS

The authors would like to acknowledge Madhu Sudhan Reddy Gudur for his suggestions. This work was supported in part by the National Institutes of Health (No. R01 EB008999).

REFERENCES

1. C. Song, B. Marshall, D. McLean et al., Proc. 27th Ann. Intl. Conf. IEEE Engin. Med. Biol. Soc., IEEE, Piscataway, NJ, USA, 2005, pp. 3456-3458.
2. V. Zderic, J. Foley, W. Luo, and S. Vaezy, *Med Phys* **35**, 4292-4299 (2008).
3. K. Ogan, W. W. Roberts, D. M. Wilhelm et al., *Urology* **62**, 146-151 (2003).
4. R. P. Madding, "Emissivity measurement using infrared imaging radiometric cameras" in *Encyclopedia of Optical Engineering, Vol. 2*, edited by R. G. Driggers, CRC, 2003, pp. 475-483.
5. D. Haemmerich, J. G. Webster, and D. M. Mahvi, Proc. 25th Ann. Intl. Conf. IEEE Engin. Med. Biol. Soc., IEEE, Pisacataway, NJ, USA, 2003, pp. 134-137.
6. V. Zderic, A. Keshavarzi, M. A. Andrew et al., *Ultrasound Med Biol* **30(1)**, 61–66 (2004).